Analysis of Subsurface Scattering under Generic Illumination

Yasuhiro Mukaigawa Kazuya Suzuki Yasushi Yagi
Osaka University, Japan
{*mukaigaw,yagi*}*@am.sanken.osaka-u.ac.jp*

Abstract

We present a new method of analyzing subsurface scattering occurring in a translucent object from a single image taken under generic illumination. In our method, diffuse subsurface reflectance in the subsurface scattering model can be linearly solved by quantizing the distances between each pair of surface points. Then, the dipole approximation is fit to the diffuse subsurface reflectance. By applying our method to real images, we confirm that the parameters of subsurface scattering can be computed for different materials.

1. Introduction

A variety of inverse rendering methods have been proposed to estimate the reflection properties of images captured by a camera. Since almost all of these assume that the target scene consists of opaque materials, translucent objects cannot be dealt with. Although marble and skin are considered typical translucent objects, many objects in our living environment such as fruit and vegetables are also translucent [1]. Recently, certain algorithms such as photon mapping [2] and dipole approximation [3] have been proposed to render translucent objects in the computer graphics field.

Translucent objects are however, not the main focus in the computer vision field. Most research is aimed at analyzing diffuse and specular reflections and shadows on opaque objects. Only inter-reflection is analyzed as an effect of global illumination. Recently, some methods have been proposed to measure subsurface scattering in translucent objects by using special lighting devices such as a laser beam [3][4][5], projector [6], and a fiber optic spectrometer [7]. However, these methods can analyze subsurface scattering under strictly controlled illumination.

In this paper, we propose a new method to analyze subsurface scattering using only a single image taken under generic illumination. Such a problem setting is difficult to solve using the previous methods.

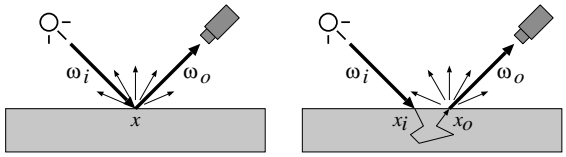

(a) Opaque object (b) Translucent object

Figure 1. BRDF and BSSRDF.

Our method analyzes subsurface scattering by fitting a dipole approximation to the captured image.

2. Subsurface Scattering

2.1. Light diffusion in translucent media

On the surface of an opaque object, an incident ray reflects directly at the incident point as shown in Fig.1(a). This reflection is expressed as a bidirectional reflectance distribution function (BRDF).

On the other hand, an incident ray to a translucent object diffuses under the surface and reflects from different points. Hence, the incident and radiative points do not correspond as shown in Fig.1(b). This reflection is expressed as a bidirectional scattering surface reflectance distribution function (BSSRDF). The BSSRDF $S(x_i, \omega_i, x_o, \omega_o)$ represents the ratio of outgoing radiance in the viewing direction ω_o at x_o to incident irradiance from a lighting direction ω_i at x_i. The radiance $L_o(x_o, \omega_o)$ is expressed by

$$L_o(x_o, \omega_o) = \int_A \int_\Omega S\left(x_i, \omega_i, x_o, \omega_o\right) L_i\left(x_i, \omega_i\right) \left(N \cdot \omega_i\right) d\omega_i \, dx_i \quad (1)$$

Here, $L_i(x_i, \omega_i)$ represents the power of the incident illumination from the direction ω_i at the surface point x_i. A, Ω, and N are the surface area, hemispherical direction, and surface normal at point x_i, respectively.

978-1-4244-2175-6/08/$25.00 ©2008 IEEE

2.2. Dipole approximation

Jensen et al. [3] proposed the dipole approximation to simulate subsurface light transport. It can render realistic images in a short time. Hence, we also use the dipole approximation to analyze translucent objects.

The dipole approximation assumes that the subsurface scattering does not depend on the incident and radiative directions. Hence, the BSSRDF $S(x_i, \omega_i, x_o, \omega_o)$ can be decomposed as

$$S(x_i, \omega_i, x_o, \omega_o) = \frac{1}{\pi} F_{t,o}(\eta, \omega_o) R(x_i, x_o) F_{t,i}(\eta, \omega_i). \quad (2)$$

Here, $F_t(\eta, \omega)$ is the Fresnel function when the ray transmits from the direction ω to the boundary whose relative index of refraction is η. $R(x_i, x_o)$ is the diffuse subsurface reflectance of light entering at point x_i and exiting at point x_o. The $R(x_i, x_o)$ is approximated to $R(d)$ as a function of the distance $d = \|x_o - x_i\|$ as follows,

$$R(d) = \frac{\alpha}{4\pi} \left\{ z_r \left(\sigma_{tr} + \frac{1}{d_r}\right) \frac{e^{-\sigma_{tr} d_r}}{d_r^2} + z_v \left(\sigma_{tr} + \frac{1}{d_v}\right) \frac{e^{-\sigma_{tr} d_v}}{d_v^2} \right\} \quad (3)$$

Each variable is defined as follows,

$$d_r = \sqrt{d^2 + z_r^2}, \quad d_v = \sqrt{d^2 + z_v^2} \quad (4)$$

$$z_r = \frac{1}{\sigma_t'}, \quad z_v = z_r\left(1 + \frac{4}{3}A\right) \quad (5)$$

$$A = \frac{1 + F_{dr}}{1 - F_{dr}} \quad (6)$$

$$F_{dr} = -\frac{1.440}{\eta^2} + \frac{0.710}{\eta} + 0.668 + 0.0636\eta \quad (7)$$

$$\sigma_{tr} = \sqrt{3\sigma_a \sigma_t'}, \quad \sigma_t' = \sigma_s' + \sigma_a, \quad \sigma_s' = \sigma_s(1 - g) \quad (8)$$

$$\alpha = \frac{\sigma_s'}{\sigma_t'} \quad (9)$$

The scattering coefficient σ_s and the absorption coefficient σ_a are inherent parameters of the material. Hence, the subsurface scattering is represented by the three parameters, σ_s, σ_a, and η.

3. Analysis of subsurface scattering

3.1. Condition

Our method estimates the parameters of the dipole approximation from only a single image taken under generic illumination. First, we clarify the condition of the proposed analyzing method as follows.

Geometry: The 3-D location of the camera and the 3-D shape of the target object are known.

Material: The material is homogeneous.

Illumination: The distribution of the illumination at each surface point $L_i(x_i, \omega_i)$ is known.

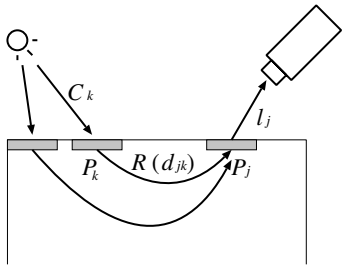

Figure 2. Formulation of radiances.

3.2. Linear formulation

The object surface is divided into m small patches and the normal vector N is calculated for each patch. The radiance $L_o(P_j)$ of patch P_j is expressed by

$$L_o(P_j) = \frac{1}{\pi} F_{t,o}(\eta, \omega_o) \sum_{k=1}^{m} \left\{ R(d_{jk}) \int_\Omega L_i(P_k, \omega_i) F_{t,i}(\eta, \omega_i) \max(0, N_k \cdot \omega_i) d\omega_i \right\}. \quad (10)$$

Here, d_{jk} denotes the length between P_j and P_k, and $L_i(P_k, \omega_i)$ denotes illuminance from the direction ω_i at P_k. We set $\eta = 1.3$ based on the research of Jensen et al. [3] and Goesele et al. [4]. Hence, $F_{t,o}(\eta, \omega_o)$ and $F_{t,i}(\eta, \omega_i)$ are calculated in advance from the 3-D shape, the illumination, and the 3-D position of the camera.

Now, we set l_j and c_k as follows

$$l_j = \pi L_o(P_j) / F_{t,o}(\eta, \omega_o), \quad (11)$$

$$c_k = \int_\Omega L_i(P_k, \omega_i) F_{t,i}(\eta, \omega_i) \max(0, N_k \cdot \omega_i) d\omega_i. \quad (12)$$

Then, l_j is represented by

$$l_j = \sum_{k=1}^{m} (R(d_{jk}) c_k), \quad (13)$$

as shown in Fig.2. By using $\mathbf{l}$, $\mathbf{c}$ and $\mathbf{R}$, defined below

$$\mathbf{l} = [l_1, l_2, \ldots, l_m]^{\mathrm{T}}, \quad \mathbf{c} = [c_1, c_2, \ldots, c_m]^{\mathrm{T}}, \quad (14)$$

$$\mathbf{R} = \begin{bmatrix} R(d_{11}) \ldots R(d_{1k}) \ldots R(d_{1m}) \\ \vdots \quad \ddots \quad \vdots \quad \vdots \\ R(d_{j1}) \ldots R(d_{jk}) \ldots R(d_{jm}) \\ \vdots \quad \vdots \quad \ddots \quad \vdots \\ R(d_{m1}) \ldots R(d_{mk}) \ldots R(d_{mm}) \end{bmatrix}, \quad (15)$$

the subsurface scattering can be expressed by the following linear formulation,

$$\mathbf{l} = \mathbf{R}\mathbf{c}. \quad (16)$$

The $\mathbf{l}$ and $\mathbf{c}$ are known, and the unknown σ_a and σ_s are included in $\mathbf{R}$. However, $\mathbf{R}$ cannot be calculated from Eq. (16) because m^2 unknowns are included in $\mathbf{R}$, while only m constraints are derived from Eq. (16).

3.3. Quantization of distance between patches

To calculate $\mathbf{R}$ from $\mathbf{l}$ and $\mathbf{c}$, we propose a linear solution. The key idea is the quantization of the distance between patches. First, the distances $d_{11}, \ldots, d_{mm}$ are approximated by n quantized distances $d'_1, d'_2, \ldots, d'_n$. R'_i denotes the diffuse subsurface reflectance corresponding to the quantized distance d'_i. The d'_i satisfy the following conditions,

$$d'_1 = 0, \quad d'_n > \max(d_{jk}), \quad (17)$$

$$d'_1 < d'_2 < \cdots < d'_n. \quad (18)$$

d_{jk} is quantized by finding i which satisfies

$$d'_i \leq d_{jk} < d'_{i+1}, \quad (19)$$

and linearly approximated by

$$d_{jk} \simeq \beta_{jk} d'_i + (1 - \beta_{jk}) d'_{i+1}, \quad (20)$$

$$\beta_{jk} = \frac{d'_{i+1} - d_{jk}}{d'_{i+1} - d'_i}. \quad (21)$$

Then, the diffuse subsurface reflectance $R(d_{jk})$ is approximated by linear interpolation as follows

$$R(d_{jk}) \simeq \beta_{jk} R'_i + (1 - \beta_{jk}) R'_{i+1}. \quad (22)$$

By using n dimensional vectors

$$\mathbf{w_{jk}} = [\cdots \quad 0 \quad \beta_{jk} \quad (1 - \beta_{jk}) \quad 0 \quad \cdots], \quad (23)$$

$$\mathbf{r} = [\, R'_1 \quad R'_2 \quad \ldots \quad R'_n \,]^{\mathrm{T}}, \quad (24)$$

Eq. (22) is represented by

$$R(d_{jk}) \simeq \mathbf{w_{jk}} \mathbf{r}. \quad (25)$$

From Eqs. (13) and (25), l_j is represented by

$$l_j \simeq \sum_{k=1}^{m} (c_k \mathbf{w_{jk}} \mathbf{r}). \quad (26)$$

Hence, Eq. (16) is approximated by

$$\mathbf{l} \simeq \mathbf{W}\mathbf{r}, \quad \mathbf{W} = \begin{bmatrix} \sum_{k=1}^{m} (c_k \mathbf{w_{1k}}) \\ \sum_{k=1}^{m} (c_k \mathbf{w_{2k}}) \\ \vdots \\ \sum_{k=1}^{m} (c_k \mathbf{w_{mk}}) \end{bmatrix}. \quad (27)$$

This equation includes n unknowns and m constraints. If $n \leq m$, $\mathbf{r}$ can be calculated linearly as

$$\mathbf{r} = \mathbf{W}^{+}\mathbf{l}. \quad (28)$$

3.4. Parameter estimation

After the diffuse subsurface reflectance R'_i has been calculated for each distance d'_i, the dipole approximation is fit to the data. $R(d)$ is uniquely decided by two parameters σ_s and σ_a. The optimal two parameters are estimated from

$$\arg\min_{\sigma_s, \sigma_a} \sum_{i=1}^{n} (R'_i - R(d'_i))^2. \quad (29)$$

4. Experiment

4.1. Simulated scene

First, we evaluated how the quantization of the distance affects the accuracy of the estimated parameters. For a precise evaluation, a simulated scene was used. Figure 3(a) shows an illumination environment [1] and (b) shows an image synthesized using the dipole approximation ($\sigma_s = 2.19$, $\sigma_a = 0.002$, $\eta = 1.3$). The parameters were estimated for each quantization step as shown in Table 1. While the estimated σ_s is similar to the ground truth, σ_a tends to be larger.

Next, the error distribution is analyzed to confirm the stability. Figure 5 shows the error distribution of all combinations of σ_s and σ_a, when the quantization distance is 0.35mm. In this figure, the values of the error are expressed by colors, and the red '+' marker indicates the estimated parameters. We can see that the

[1] http://www.debevec.org/Probes/

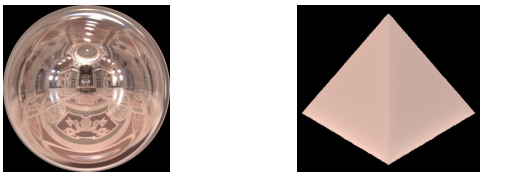

(a) illumination environment (b) synthesized image

Figure 3. Simulated scene.

Table 1. Estimated parameters and PSNR.

Sampling[mm]	σ_s	σ_a	PSNR [dB]
0.05	2.14	0.000	26.47
0.10	2.20	0.007	42.12
0.15	2.19	0.004	30.58
0.20	2.19	0.009	33.47
0.25	2.19	0.005	28.69
0.30	2.32	0.009	29.78
0.35	2.34	0.009	47.93
0.40	2.22	0.009	25.76
0.45	2.18	0.009	20.35
0.50	2.40	0.009	23.43
Ground truth	2.19	0.002	-

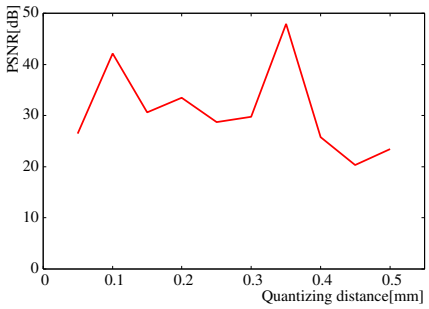

Figure 4. Relationship between quantizing distance and PSNR.

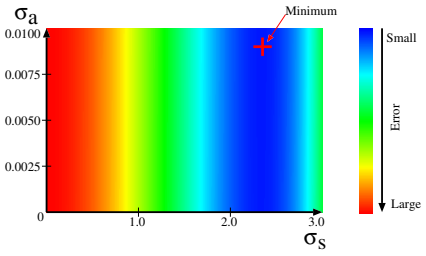

Figure 5. Error distribution when quantizing distance is 0.35mm.

obvious minimum exists for σ_s and that the estimation of σ_s is stable. On the other hand, the error does not vary even if σ_a changes. That is, the estimation of σ_a tends to be unstable. In fact, $R(d)$ does not dramatically change when σ_a varies. Figure 6 shows the fitting result when the quantization distance is 0.35mm. Although the estimated $R(d)$ is slightly small due to some outliers, almost correct $R(d)$ is estimated.

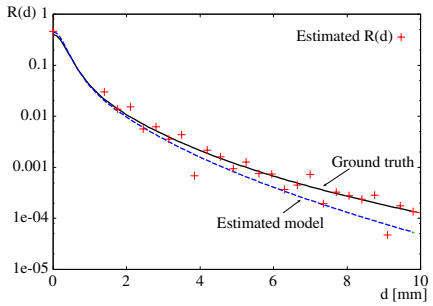

Figure 6. Fitting result when quantizing distance is 0.35mm.

4.2. Real scene

Next, the parameters were estimated from real images. The images were captured by a Nikon D80 digital camera as shown in Fig. 7. The illumination is a white LED and the 3-D position is measured precisely by the Leica total station. The cube and pyramid objects are made of three different materials; polypropylene (PP), polyethylene (PE), and polyoxymethylene (POM). Each object is captured under two illumination conditions. In total, 12 images (2 shapes $\times$ 3 materials $\times$ 2 illuminations) were captured as shown in Fig. 8.

By changing the quantization distance, the optimal parameters were estimated for each image as shown in Table 2 and Fig.9. Ideally, the same parameters should be estimated for the same material. While the estimation of σ_a is slightly unstable, similar values of σ_s are estimated for each material, with the exception of the cube under illumination 1.

Figure 10 shows $R(d)$ for each material calculated by the average of the estimated parameters. By using the estimated $R(d)$, the Stanford bunnies are rendered as shown in Fig. 11. We can see that different subsurface scattering is expressed.

5. Conclusion

We proposed a new method to analyze subsurface scattering from a single image taken under generic illumination. We showed that diffuse subsurface reflectance can be linearly calculated by quantizing the distances between each pair of surface points. Although the analysis is not stable, we believe that our method is

Figure 7. Real scene.

(a) polypropylene (PP)

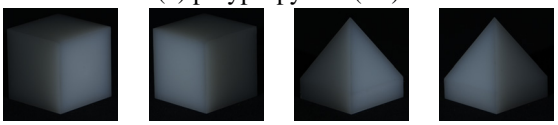

(b) polyethylene (PE)

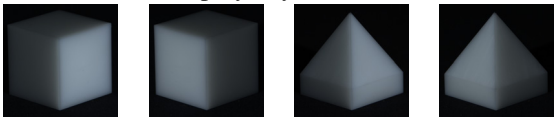

(c) polyoxymethylene (POM)

Figure 8. Real translucent objects.

Table 2. Estimated parameters.

material	shape	illumination	σ_s	σ_a
PP	cube	1	2.62	0.010
		2	1.69	0.000
	pyramid	1	2.07	0.010
		2	2.12	0.010
PE	cube	1	0.01	0.001
		2	0.08	0.001
	pyramid	1	0.28	0.000
		2	0.15	0.010
POM	cube	1	0.03	0.000
		2	0.37	0.010
	pyramid	1	0.56	0.010
		2	0.37	0.010

a significant first step in the inverse rendering of translucent objects.

This work is supported by the Special Coordination Funds for Promoting Science and Technology of Ministry of Education, Culture, Sports, Science and Technology.

References

[1] S. K. Nayar, G. Krishnan, M. D. Grossberg, and R. Raskar, "Fast Separation of Direct and Global Components of a Scene using High Frequency Illumination", Proc. SIGGRAPH2006 pp.935-944, 2006.

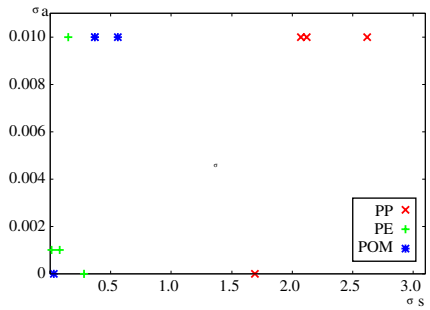

Figure 9. Parameters for each material.

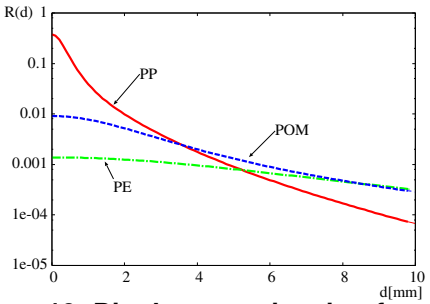

Figure 10. Dipole approximation for each material.

(a) PP (b) PE (c) POM

Figure 11. Rendered Stanford bunnies.

[2] H. W. Jensen, "Realistic Image Synthesis using Photon Mapping", ISBN: 1-56881-140-7, AK Peters, 2001.

[3] H. W. Jensen, S. R. Marschner, M. Levoy, and P. Hanrahan, "A Practical Model for Subsurface Light Transport", Proc. SIGGRAPH2001, pp.511-518, 2001.

[4] M. Goesele, H. P. A. Lensch, J. Lang, C. Fuchs, and H. P. Seidel, "Disco - Acquisition of Translucent Objects", Proc. SIGGRAPH2004, pp.835-844, 2004.

[5] C. Fuchs, M. Goesele, T. Chen, H. P. Seidel, "An Empirical Model for Heterogeneous Translucent Objects", Research Report MPI-I-2005-4-006, 2005.

[6] S. Tariq, A. Gardner, I. Llamas, A. Jones, P. Debevec, and G. Turk, "Efficient Estimation of Spatially Varying Subsurface Scattering Parameters", Vision, Modeling, and Visualization (VMV2006), 2006.

[7] T. Weyrich, W. Matusik, H. Pfister, B. Bickel, C. Donner, C. Tu, J. McAndless, J. Lee, A. Ngan, H. W. Jensen, and M. Gross, "Analysis of Human Faces using a Measurement-Based Skin Reflectance Model", Proc. SIGGRAPH2006, pp.1013-1024, 2006.